physical sciences forum

Proceeding Paper

Isospin Symmetry Breaking in Non-Perturbative QCD

Abdel Nasser Tawfik

MDPI

https://doi.org/10.3390/ECU2023-14047

physical sciences forum

MDPI

Proceeding Paper

Isospin Symmetry Breaking in Non-Perturbative QCD †

Abdel Nasser Tawfik

Research Center, Faculty of Engineering, Future University in Egypt (FUE), End of 90th Street, Fifth Settlement, New Cairo 12835, Egypt; a.tawfik@fue.edu.eg

† Presented at the 2nd Electronic Conference on Universe, 16 February–2 March 2023; Available online: https://ecu2023.sciforum.net/.

Abstract: At finite isospin chemical potential μ_I, the tension between measured decays and partial branching ratios of neutral and charged bosons as functions of dimuon mass squared and the Standard Model (SM) isospin asymmetry can be analyzed in nonperturbative QCD-effective models, for instance, the Polyakov linear sigma-model. With almost first-principle derivation of the explicit isospin symmetry breaking, namely, $\bar{\sigma}_3 = f_{K^\pm} - f_{K^0}$ the isospin sigma field, and $h_3 = m_{a_0}^2 (f_{K^\pm} - f_{K^0})$ the third generator of the matrix of the explicit symmetry breaking $H = T_a h_a$. $f_{K^\pm}$ and f_{K^0} are decay constants of $K^\pm$ and K^0, respectively. m_{a_0} is the mass of a_0 meson. Accordingly, the QCD phase structure could be extended to finite μ_I. With the thermal and density dependence of a_0, $f_{K^\pm}$, and f_{K^0}, $\bar{\sigma}_3$ and h_3 are accordingly expressed in dependence on the temperatures and the chemical potentials. We find that the resulting critical chiral temperatures T_χ decrease with the increase in μ_B and/or μ_I. We conclude that the $(T_\chi - \mu_I)$ boundary has almost the same structure as that of the $(T_\chi - \mu_B)$ plane.

Keywords: chiral symmetries; chiral transition; chiral Lagrangian; isobaric spin

PACS: 11.30.Rd; 11.10.Wx; 12.39.Fe; 21.10.Hw

1. Introduction

At finite isospin chemical potential μ_I, the lattice Quantum ChromoDynamics (QCD) simulations have real and positive action so that the Monte Carlo (MC) techniques are well applicable [1]. On the other hand, at finite baryon chemical potential μ_B, the action becomes complex, i.e., sign problem [2]. Both types of nonperturbative simulations share common features, for example, deconfinement, hadronization, hadron-parton phase transition, Silverblaze phenomenon, and Bose–Einstein condensations. Hence, even qualitative if not quantitative conclusions on nonperturbative QCD, at finite μ_I, are of great importance [3]. This might go beyond the current limitations and offer a theoretical framework for the Bose–Einstein condensations and the yet-still-hypothetical superconducting phases [4]. Thereby, the QCD phase diagram is enriched [5]. Characterizing the possible imbalance between the charged pions degrees-of-freedom [6] in dense quark matter, such as the neutron stars [7,8], is an astrophysical example of the chiral isospin asymmetry.

The QCD-like effective models, such as the Ployakov linear-sigma model (PLSM), offer a complementary approach to the nonperturbative QCD [9–12]. The present script introduces a novel study suggesting first-principle derivations of a new set of PLSM parameters, namely, h_3 and $bar\sigma_3$ the isospin sigma field. As a result of the spontaneous symmetry breaking in the QCD-like effective nonperturbative QCD approach, the PLSM, the mean value of the field Φ, $\langle\Phi\rangle$, and that of its conjugate $\langle\Phi^\dagger\rangle$ could be related to the quantum numbers of the vacuum [13]. Therefore, while the mean values of $\bar{\pi}_a$ vanish, that of the quark condensates $\bar{\sigma}_a$ remain finite. Concretely, $\bar{\sigma}_0 \neq \bar{\sigma}_3 \neq \bar{\sigma}_8 \neq 0$ corresponding to the diagonal generators $U(3)$. On the other hand, the isospin symmetry is broken in SU(2) though finite quark condensates $\bar{\sigma}_3$ [13] and finite $\mathrm{Tr}[H(\Phi + \Phi^\dagger)$ in the PLSM Langrangian. Thus, the symmetry generators h_a are conjectured to break the isospin

check for updates

Citation: Tawfik, A.N. Isospin Symmetry Breaking in Non-Perturbative QCD. *Phys. Sci. Forum* **2023**, *7*, 22. https://doi.org/10.3390/ECU2023-14047

Academic Editor: Jin Min Yang

Published: 16 February 2023

symmetry, as $H = T_a h_a$. Therefore, the finite diagonal components of h_0, h_3, h_8 lead to finite condensates $\bar{\sigma_0}$, $\bar{\sigma_3}$ and $\bar{\sigma_8}$ corresponding to the three quark flavors. Accordingly, the masses of the three quark flavors are no longer degenerate, i.e., $m_u \neq m_d \neq m_s$. It is obvious that the nature likely prefers such a configuration. By converting the three quark condensates through the orthogonal basis transformation from the original basis, σ_0, σ_3, and σ_8 to pure up (σ_u), down (σ_d), and strange (σ_s) quark flavor basis, we obtain,

$$\begin{bmatrix} \bar{\sigma_u} \\ \bar{\sigma_d} \\ \bar{\sigma_s} \end{bmatrix} = \frac{1}{\sqrt{3}} \begin{bmatrix} \sqrt{2} & 1 & 1 \\ \sqrt{2} & -1 & 1 \\ 1 & 0 & -\sqrt{2} \end{bmatrix} \begin{bmatrix} \bar{\sigma_0} \\ \bar{\sigma_3} \\ \bar{\sigma_8} \end{bmatrix}. \tag{1}$$

In light of this, the masses of u-, d-, and s-quarks can be expressed as,

$$m_u = \frac{g}{2}\sigma_u, \qquad m_d = \frac{g}{2}\sigma_d, \qquad m_s = \frac{g}{\sqrt{2}}\sigma_s. \tag{2}$$

In the present calculations, we introduce PLSM calculations for the thermodynamic properties and thereby the chiral QCD phase structure, at finite isospin asymmetry. Firstly, the effects of finite isospin asymmetry on differentiation between the nonstrange (light) condensates of u- and d-quark shall be analyzed. Secondly, as a result of the isospin symmetry breaking, $\bar{\sigma_3}$ should have a nonzero value because $\sigma_u = \sigma_l + \sigma_3$ and $\sigma_d = \sigma_l - \sigma_3$. To this end, we estimate the pure mesonic potential for N_f quark flavors, Equation (14), as functions of temperatures and chemical potentials.

To the author's best knowledge, there is so-far no reliable estimation for the generator h_3. Following the assumption of refs. [14,15], we first assume that the violation of the isospin symmetry is negligibly small, i.e., $h_3 \to 0$, see Table 1. In this limit, one assumes that the u- and d-quark condensates can be given as $\sigma_u = \sigma_l + \sigma_3$ and $\sigma_d = \sigma_l - \sigma_3$, where σ_l is the nonstrange light condensate $\sigma_l = (\sigma_u + \sigma_d)/2$ for non-degenerated masses of the light quarks, Equation (1). The main contribution of the present script is revising such an assumption. Finite h_3, the third generator of the matrix of the explicit symmetry breaking $H = T_a h_a$, and $\bar{\sigma_3}$, the isospin sigma field, considerably contribute to the isospin symmetry breaking. We are not just assigning finite values to h_3 and $\bar{\sigma_3}$. We rather introduce a theoretical framework for the thermal and dense dependence of both h_3 and $\bar{\sigma_3}$.

Table 1. Various LSM parameters fixed at $m_\sigma = 800$ MeV and $h_3 = 0$ [16].

m_σ [MeV]	c [MeV]	h_{ud} [MeV^3]	h_3 [MeV^3]	h_s [MeV^3]	m^2 [MeV^2]	λ_1	λ_2
800	4807.84	$(120.73)^3$	0	$(336.41)^3$	$-(306.26)^2$	13.49	46.48

The present script is organized as follows. In Section 2, the formalism is outlined. The effective nonperturbative QCD approach, the SU(3) Polyakov linear-sigma model (PLSM), at vanishing h_3, is introduced in Section 2.1. The isospin symmetry breaking based on suggesting finite h_3 is discussed in Section 2.2. In Section 3, we investigate the impacts of the isospin asymmetry on the QCD phase transition(s). Last but not least, Section 4 is devoted to the conclusions.

2. Formalism

The limitation of the MC techniques to vanishing baryon chemical potential in the non-perturbative lattice QCD promotes the utilization of QCD-like effective approaches. In the present study, we focus on the Polyakov linear-sigma model (PLSM). Various QCD quantities, including the thermodynamics of conserved charges and chiral quark-hadron phase transitions, can be estimated at least qualitatively [15,17–25].

Here, we aim at analyzing how the finite isospin asymmetry should be integrated in the chiral models, PLSM, especially that the nonperturbative lattice QCD simulations—in contrast to the finite baryon chemical potential—are reliable, at finite isospin chemical

potential. Having done this allows the characterization of the thermodynamic properties of the nonperturbative QCD and thereby the mapping out of the QCD phase diagram. With finite isospin asymmetry, the generic chemical potentials of both light quarks are no longer degenerate. The PLSM thermodynamics in thermal and dense medium shall be confronted to the recent lattice QCD simulations. To this end, we aim at presenting a general expression of the chiral limit, at finite isospin asymmetry.

2.1. PLSM at Finite Chemical Potential

In flat Minkowski space, the Lagrangian of the linear-sigma model (LSM) with N_f quark flavors and Polyakov-loop potential would be summarized as

$$\mathcal{L}_{PLSM} = \mathcal{L}_{\psi} + \mathcal{L}_{m} - \mathcal{U}(\phi, \bar{\phi}, T), \tag{3}$$

where $\mathcal{L}_{\psi}$ represent the quarks (fermions), while $\mathcal{L}_{m}$ represents the mesons (bosons), and $\mathcal{U}(\phi, \bar{\phi}, T)$ represents the Polyakov-loop potential contributions. For N_c, the color degrees of freedom, the contributions of the quarks (fermions) read

$$\mathcal{L}_{\psi} \quad = \quad \sum_{f} \overline{\psi}_f (i\gamma^{\mu} D_{\mu} - g\, T_a(\sigma_a + i\gamma_5 \pi_a))\psi_f, \tag{4}$$

where ψ are the Dirac spinor fields; $f = [u,\, d,\, s]$ are the quark flavors; and D_{μ}, μ, γ^{μ} and g, respectively, represent the covariant derivative, Lorentz index, chiral spinors, and Yukawa coupling constant. The contributions of the mesons (bosons) are given as,

$$\begin{aligned} \mathcal{L}_{m} \quad &= \quad \mathrm{Tr}(\partial_{\nu}\Phi^{\dagger}\partial^{\nu}\Phi - m^2\Phi^{\dagger}\Phi) - \lambda_1\,[\mathrm{Tr}\,(\Phi^{\dagger}\Phi)]^2 \\ &- \quad \lambda_2\,\mathrm{Tr}(\Phi^{\dagger}\Phi)^2 + c[\mathrm{Det}(\Phi) + \mathrm{Det}(\Phi^{\dagger})] + \mathrm{Tr}[H(\Phi + \Phi^{\dagger})], \end{aligned} \tag{5}$$

where Φ is the nonet meson (3×3)-matrix,

$$\bar{\Phi} \quad = \quad \sum_{a=0}^{N_f^2-1} T_a(\bar{\sigma_a} + i\bar{\pi}_a). \tag{6}$$

and $T_a = \hat{\lambda}_a/2$ is a generator operator in U(3) algebra. T_a can be determined from the Gell–Mann matrices $\hat{\lambda}_a$ with $a = 0, \cdots, 8$ [26].

So far, we have various LSM parameters to be fixed, namely, m^2, h_l, h_s, λ_1, λ_2, and c. They are strongly dependent on the mass of the sigma meson m_{σ} [16]. In the present calculations, we assumed that $m_{\sigma} = 800$ MeV. Table 1 summarizes all these parameters [16]. The present script aims at determining another set of parameters, namely, h_3 and $\bar{\sigma}_3$, the third generator of the matrix of the explicit symmetry breaking H and isospin sigma field, respectively. In this regard, we recall that the same symbol h_3 was used in refs. Refer to [27,28] for the dimensionless coupling constant distinguishing between u and d quark flavors.

The third type of contributions to the PLSM Lagrangian, Equation (3), represents the Polyakov-loop potential responsible for the gluonic degrees of freedom and the dynamics of the quark-gluon interactions, $\mathcal{U}(\phi, \bar{\phi}, T)$. The Polyakov-loop potentials are suggested to characterize the QCD symmetries in pure-gauge theory [18,19,23,29,30]. For example, based on strong coupling simulations and by including higher-order Polyakov-loop variables, we have

$$\mathcal{U}_{\mathrm{Fuku}}(\phi, \bar{\phi}, T) \quad = \quad -b\,T\Big[54\,\phi\,\bar{\phi}\;\exp(-a/T) + \ln(1 - 6\phi\bar{\phi} - 3(\phi\bar{\phi})^2 + 4(\phi^3 + \bar{\phi}^3))\Big]. \tag{7}$$

In temporal space, the thermal expectation value of the color traced Wilson loop, also known as the Polyakov-loop variable, reads

$$\phi = (\mathrm{Tr}_c\,\mathcal{P})/N_c, \tag{8}$$
$$\bar{\phi} = (\mathrm{Tr}_c\,\mathcal{P}^\dagger)/N_c, \tag{9}$$

where $\mathcal{P}$ are the Polyakov loops.

Then, in the mean-field approximation, the PLSM grand-canonical potential can be expressed as

$$\Omega(T,\mu_f) = \frac{-T\cdot\ln[\mathcal{Z}]}{V} = \Omega_{\bar{\psi}\psi}(T,\,\mu_f) + U(\sigma_u,\,\sigma_d,\,\sigma_s) + \mathcal{U}_{\mathrm{Fuku}}(\phi,\bar{\phi},T), \tag{10}$$

where μ_f are the chemical potentials of the three quark flavors. For the conserved charge baryon B, strangeness S, electric charge Q, and isospin I, the quark chemical potentials are composed as

$$\mu_u = \frac{\mu_B}{3} + \frac{2\mu_Q}{3} + \frac{\mu_I}{2}, \tag{11}$$
$$\mu_d = \frac{\mu_B}{3} - \frac{\mu_Q}{3} - \frac{\mu_I}{2}, \tag{12}$$
$$\mu_s = \frac{\mu_B}{3} - \frac{\mu_Q}{3} - \mu_S, \tag{13}$$

accordingly, the mesonic contributions to the LSM potential $U(\sigma_u,\,\sigma_d,\,\sigma_s)$ can be determined by substituting Equation (6), the mesonic field, into Equation (5)

$$\begin{aligned} U(\sigma_u,\,\sigma_d,\,\sigma_s) &= \frac{m^2}{4}\left[\sigma_u^2+\sigma_d^2+2\sigma_s^2\right] - \frac{c}{2\sqrt{2}}\sigma_u\,\sigma_d\,\sigma_s + \frac{\lambda_1}{16}\left(\sigma_u^2+\sigma_d^2+2\sigma_s^2\right)^2 \\ &+ \frac{\lambda_2}{16}\left(\sigma_u^4+\sigma_d^4+4\sigma_s^4\right) - h_{ud}\frac{\sigma_u+\sigma_d}{2} - h_3\frac{\sigma_u-\sigma_d}{2} - h_s\sigma_s, \end{aligned} \tag{14}$$

where h_3 shall be derived in Section 2.2.

The contributions of quarks and antiquarks to the PLSM potential are given as [18,31–33]

$$\Omega_{\bar{\psi}\psi}(T,\mu_f) = -2\,T\sum_{f=u,d,s}\int_0^\infty \frac{d^3\vec{P}}{(2\pi)^3}\ln\left[1+n_{q,f}(T,\,\mu_f)\right] + \ln\left[1+n_{\bar{q},f}(T,\,\mu_f)\right]. \tag{15}$$

It is evident that $n_{\bar{q},f}(T,\,\mu_f)$ is identical to $n_{q,f}(T,\,\mu_f)$ with a double replacement, namely, $-\mu_f$ by $+\mu_f$ and the order parameter of the Ployakov-loop field ϕ by its conjugate $\bar{\phi}$ or vice versa.

$$n_{q,f}(T,\,\mu_f) = 3\left(\phi+\bar{\phi}e^{-\frac{E_f-\mu_f}{T}}\right)\times e^{-\frac{E_f-\mu_f}{T}} + e^{-3\frac{E_f-\mu_f}{T}}. \tag{16}$$

$E_f = (\vec{P}^2+m_f^2)^{1/2}$ gives the energy-momentum dispersion relation corresponding to the quark and antiquark, where m_f is the mass of fth quark flavor. Equation (10) expresses the grand canonical potential, which in mean-field approximation derives the various physical quantities characterizing the QCD thermodynamics and thereby the QCD phase structure in thermal and dense medium.

2.2. Isospin Asymmetry and Meson Potential

As discussed in the previous section, the isospin asymmetry SU(2) is broken, at finite $\bar{\sigma}_3$ [13], not only $\bar{\sigma}_3$, which breaks the isospin symmetry, but also the potential of pure mesonic contributions in SU(N_f), which can be rewritten as [14],

$$U(\bar{\sigma}) = \left(\frac{m^2}{2} - h_a\right)\bar{\sigma}_a - 3\mathcal{G}_{abc}\bar{\sigma}_b\,\bar{\sigma}_c - \frac{4}{3}\mathcal{F}_{abcd}\,\bar{\sigma}_b\,\bar{\sigma}_c\bar{\sigma}_d, \tag{17}$$

where the coefficients $\mathcal{G}_{abc}$ and $\mathcal{F}_{abcd}$ are given as [14]

$$\mathcal{G}_{abc} = \frac{c}{6}\left[d_{abc} - \frac{3}{2}(d_{0bc}\delta_{a0} + d_{a0c}\delta_{b0} + d_{ab0}\delta_{c0}) + \frac{9}{2}d_{000}\delta_{a0}\delta_{b0}\delta_{c0}\right], \tag{18}$$

$$\mathcal{F}_{abcd} = \frac{\lambda_1}{4}[\delta_{ab}\delta_{cd} + \delta_{ad}\delta_{cd} + \delta_{ac}\delta_{bd}] + \frac{\lambda_2}{8}[d_{abn}d_{ncd} + d_{adn}d_{nbc} + d_{acn}d_{nbd}]. \tag{19}$$

We notice that the explicitly symmetry breaking terms, h_0, h_3, and h_8, can be determined by minimizing the potential, Equation (17), on tree level, $\partial U(\bar{\sigma})/\partial\bar{\sigma}_a = 0$. Concretely, both h_0 and h_8 can be determined from the partially conserved axial current (PCAC) relations.

The generator operator $\hat{T}_a = \hat{\lambda}_a/2$ in U(3) is obtained from Gell–Mann matrices $\hat{\lambda}_a$ [26] with the indices running as $a = 0, \cdots, 8$. From U(3) algebra, we have

$$[\hat{T}_a,\ \hat{T}_b] = if_{abc}\hat{T}_c, \tag{20}$$

$$\{\hat{T}_a,\ \hat{T}_b\} = id_{abc}\hat{T}_c, \tag{21}$$

where f_{abc} and d_{abc}, respectively, are the standard antisymmetric and symmetric structure constants of SU(3). In this regard, the symmetric structure constant d_{abc} can be defined as

$$d_{abc} = \frac{1}{4}Tr[\{\hat{\lambda}_a,\ \hat{\lambda}_b\}\hat{\lambda}_c], \tag{22}$$

$$d_{ab0} = \sqrt{\frac{2}{3}}\,\delta_{ab}. \tag{23}$$

In PCAC relation, the decay constant f_a is related to the symmetric structure constant as

$$f_a = d_{aab}\bar{\sigma}_a. \tag{24}$$

Accordingly, the decay constants of the charged and neutral pion mesons ($f_{\pi^\pm} = f_1$, $f_{\pi^0} = f_3$) and the kaon meson ($f_{K^\pm} = f_4$, $f_{K^0} = f_6$) are given as

$$f_{\pi^0} = f_{\pi^\pm} = \sqrt{\frac{2}{3}}\bar{\sigma}_0 + \frac{1}{\sqrt{3}}\bar{\sigma}_8, \tag{25}$$

$$f_{K^\pm} = \sqrt{\frac{2}{3}}\bar{\sigma}_0 + \frac{1}{2}\bar{\sigma}_3 - \frac{1}{2\sqrt{3}}\bar{\sigma}_8, \tag{26}$$

$$f_{K^0} = \sqrt{\frac{2}{3}}\bar{\sigma}_0 - \frac{1}{2}\bar{\sigma}_3 - \frac{1}{2\sqrt{3}}\bar{\sigma}_8, \tag{27}$$

where the isospin sigma field, $\bar{\sigma}_3$, is the difference between the decay constants of neutral and charged kaon mesons as

$$\bar{\sigma}_3 = f_{K^\pm} - f_{K^0}. \tag{28}$$

From the experimental and recent lattice review on physical constants [34–36], $f_{\pi^\pm} = f_{\pi^0} = 92.4$ MeV and $f_{K^\pm} = 113$ MeV, $f_{K^0} = 113.453$ MeV. Then, we suggest expressions for both h_0 and h_8,

$$h_0 = \frac{1}{\sqrt{6}}\Big(m_\pi^2 f_\pi + 2m_K^2 f_K\Big), \tag{29}$$

$$h_8 = \frac{2}{\sqrt{3}}\Big(m_\pi^2 f_\pi - m_K^2 f_K\Big). \tag{30}$$

The explicit symmetry breaking term, h_3, the third generator of the matrix of the explicit symmetry breaking $H = T_a h_a$, can be deduced from $\partial U(\bar{\sigma})/\partial\bar{\sigma}_3 = 0$,

$$h_3 = \Bigg[m^2 + \frac{c}{\sqrt{6}}\bar{\sigma}_0 - \frac{c}{\sqrt{3}}\bar{\sigma}_8 + \lambda_1\Big({\bar{\sigma}_0}^2 + {\bar{\sigma}_3}^2 + {\bar{\sigma}_8}^2\Big) + \lambda_2\Big({\bar{\sigma}_0}^2 + \frac{{\bar{\sigma}_3}^2}{2} + \frac{{\bar{\sigma}_8}^2}{2} + \sqrt{2}\bar{\sigma}_0\bar{\sigma}_8\Big)\Bigg]\bar{\sigma}_3, \tag{31}$$

where the square brackets $[\cdots]$ is the squared mass of the a_0 meson, Equation (28). Then, h_3 can be expressed as

$$h_3 = m_{a_0}^2(f_{K^\pm} - f_{K^0}), \tag{32}$$

As discussed in the Introduction, the finite isospin asymmetry leads to degenerate masses of the quark flavors, namely, $m_u \neq m_d \neq m_s$. At nonvanishing h_3, the PLSM parameters listed in Table 1 are revised, Table 2.

Table 2. The revised values of the LSM parameters, Equation (5), at $m_\sigma = 800$ MeV [16].

m_σ [MeV]	c [MeV]	h_{ud} [MeV^3]	h_3 [MeV^3]	h_s [MeV^3]	m^2 [MeV^2]	λ_1	λ_2
800	4807.84	$(120.73)^3$	$-(78.31)^3$	$(336.41)^3$	$-(306.26)^2$	13.49	46.48

3. Results and Discussion

For a reliable differentiation between u- and d-quark condensates, the influences of the finite isospin asymmetry on the corresponding PLSM chiral condensates and on the deconfinement order parameters should be estimated [37]. It was pointed out that the impacts of finite isospin asymmetry enhances the PLSM thermodynamics, especially with the increase in temperatures. The dependence of the PLSM critical chiral temperatures on the isospin asymmetry obviously maps out the QCD phase structure. The critical chiral temperature decreases as the isospin asymmetry increases. We also conclude that the PLSM results on the critical temperatures reproduce the recent lattice QCD simulations well [38,39], Figure 1 For a reliable comparison, both temperature and isospin chemical potential are normalized to the critical temperature and the pion mass, respectively, as follows. For lattice QCD: $m_\pi = 400.0$ MeV and $T_\chi^{\mu_I=0} = 164$ MeV. For PLSM: $m_\pi = 138$ MeV and $T_\chi^{\mu_I=0} = 210$ MeV.

At finite μ_I, the potential impacts of $bar\sigma_3$ and h_3 are taken into consideration. The procedure to determine the critical chiral temperature goes as follows.

- Both u- and d-quark chiral condensates become distinguishable. As the temperature approaches a critical value, the normalized nonstrange condensates are split into two different curves. At this point, the critical chiral temperatures, T_χ, can be at least qualitatively estimated. We notice that the value of the resulting T_χ decreases with increasing μ_I.
- Both Ployakov-loop variables ϕ and $\bar{\phi}$ also become distinguishable. Increasing μ_I decreases $\bar{\phi}$ but increases ϕ. Moreover, both ϕ and $\bar{\phi}$ become more distinguishable with a further increase in μ_I.

- Both nonstrange quark susceptibilities become distinguishable as well. The critical chiral temperature T_χ is positioned in the middle of the deconfinement phase transition. The resulting T_χ decreases with the increase in μ_I.

The Figure 1 illustrates that similar to the lattice QCD simulations [38,39], the critical temperature decreases with increasing μ_I. Because the PLSM results reproduce the available lattice QCD calculations well, it is possible to predict the tendency at larger μ_I. Furthermore, when comparing our results for Figure 1, with the QCD phase structure in (T_χ-μ_B) plane reported in refs. [10,40–42], good similarity can be concluded.

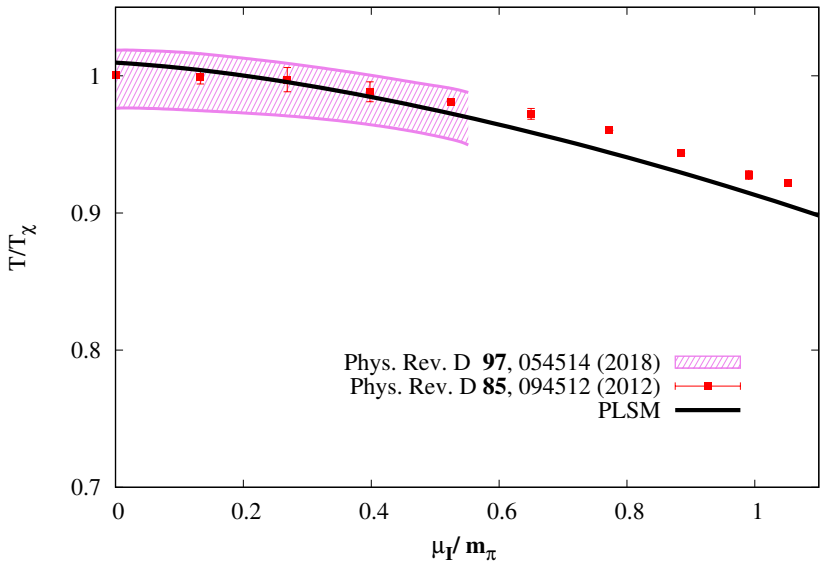

Figure 1. The QCD phase diagram at vanishing baryon chemical potential but finite isospin chemical potential. The PLSM results (solid curves) are confronted to recent lattice QCD calculations (symbols) [38,39].

4. Conclusions

We have studied the Ployakov linear-sigma model with three quark flavors and $U(1)_A$ anomaly, at finite isospin asymmetry. The finite isospin asymmetry emerges nonvanishing diagonal generators $\sigma_0 \neq \sigma_3 \neq \sigma_8 \neq 0$ of the mean sigma-fields $\bar{\sigma_a}$. This means that the $SU(2)$ isospin asymmetry is broken through σ_3, i.e., $\sigma_u = \sigma_l + \sigma_3$ and $\sigma_d = \sigma_l - \sigma_3$ [14,43,44].

From the thermal and dense dependence of the quark condensates σ_u, σ_d, and σ_s, and the Polyakov-loop variables ϕ and $\bar{\phi}$, fruitful information, especially about the QCD chiral phase transition, becomes available. All of these quantities can be estimated by minimizing the real part of thermodynamic potential, $\mathcal{R}e\,[\Omega(T,\,\mu_f)]$, Equation (10). We conclude the chiral QCD phase transition, the dependence of the critical chiral temperatures on the isospin chemical potential, looks very similar to the QCD phase transition, the dependence of the critical temperatures on the baryon chemical potential, i.e., the (T_χ-μ_I) plane looks very similar to the (T_χ-μ_B) plane. We conclude that the critical chiral temperatures are not universally constant. This apparently depends on the quark flavors and the isospin chemical potentials.

Funding: This research received no external funding.

Data Availability Statement: All types of relevant data are included in the manuscript.

Conflicts of Interest: The author declares no conflict of interest.

References

1. Son, D.T.; Stephanov, M.A. QCD at finite isospin density. *Phys. Rev. Lett.* **2001**, *86*, 592. [CrossRef]
2. Philipsen, O. Lattice QCD at finite temperature and density. *Eur. Phys. J. Spec. Top.* **2007**, *152*, 29. [CrossRef]
3. Brandt, B.B.; Endrodi, G.; Schmalzbauer, S. QCD phase diagram for nonzero isospin-asymmetry. *EPJ Web Conf.* **2018**, *175*, 07020. [CrossRef]
4. Detmold, W.; Orginos, K.; Shi, Z. Lattice QCD at non-zero isospin chemical potential. *Phys. Rev.* **2012**, *D86*, 054507.
5. Tawfik, A. QCD phase diagram: A Comparison of lattice and hadron resonance gas model calculations. *Phys. Rev. D* **2005**, *71*, 054502. [CrossRef]
6. Li, B.-A.; Ko, C.M.; Bauer, W. Isospin physics in heavy ion collisions at intermediate-energies. *Int. J. Mod. Phys.* **1998**, *E7*, 147. [CrossRef]
7. Migdal, A.B.; Saperstein, E.E.; Troitsky, M.A.; Voskresensky, D.N. Pion degrees of freedom in nuclear matter. *Phys. Rep.* **1990**, *192*, 179. [CrossRef]
8. Steiner, A.W.; Prakash, M.; Lattimer, J.M.; Ellis, P.J. Isospin asymmetry in nuclei and neutron stars. *Phys. Rep.* **2005**, *411*, 325. [CrossRef]
9. Abdel Aal Diab, A.M.; Tawfik, A.N. Quark-hadron phase structure of QCD matter from SU(4) Polyakov linear sigma model. *EPJ Web Conf.* **2018**, *177*, 09005. [CrossRef]
10. Tawfik, A.N.; Diab, A.M.; Hussein, M.T. Quark-hadron phase structure, thermodynamics, and magnetization of QCD matter. *J. Phys.* **2018**, *G45*, 055008. [CrossRef]
11. Tawfik, A.N.; Magdy, N. SU(3) Polyakov linear-σ model in magnetic fields: Thermodynamics, higher-order moments, chiral phase structure, and meson masses. *Phys. Rev.* **2015**, *C91*, 015206.
12. Tawfik, A.N.; Diab, A.M. Polyakov SU(3) extended linear-σ model: Sixteen mesonic states in chiral phase structure. *Phys. Rev.* **2015**, *C91*, 015204.
13. Gasiorowicz, S.; Geffen, D.A. Effective Lagrangians and field algebras with chiral symmetry. *Rev. Mod. Phys.* **1969**, *41*, 531. [CrossRef]
14. Lenaghan, J.T.; Rischke, D.H.; Schaffner-Bielich, J. Chiral symmetry restoration at nonzero temperature in the SU(3)(r) x SU(3)(l) linear sigma model. *Phys. Rev.* **2000**, *D62*, 085008.
15. Rischke, D.H. The Quark gluon plasma in equilibrium. *Prog. Part. Nucl. Phys.* **2004**, *52*, 197. [CrossRef]
16. Schaefer, B.-J.; Wagner, M. The Three-flavor chiral phase structure in hot and dense QCD matter. *Phys. Rev.* **2009**, *D79*, 014018. [CrossRef]
17. Asakawa, M.; Yazaki, K. Chiral Restoration at Finite Density and Temperature. *Nucl. Phys.* **1989**, *A504*, 668.
18. Fukushima, K. Phase diagrams in the three-flavor Nambu–Jona–Lasinio model with the Polyakov loop. *Phys. Rev.* **2008**, *D77*, 114028. [CrossRef]
19. Ratti, C.; Thaler, M.A.; Weise, W. Phases of QCD: Lattice thermodynamics and a field theoretical model. *Phys. Rev.* **2006**, *D73*, 014019. [CrossRef]
20. Carignano, S.; Nickel, D.; Buballa, M. Influence of vector interaction and Polyakov loop dynamics on inhomogeneous chiral symmetry breaking phases. *Phys. Rev.* **2010**, *D82*, 054009. [CrossRef]
21. Bratovic, N.M.; Hatsuda, T.; Weise, W. Role of Vector Interaction and Axial Anomaly in the PNJL Modeling of the QCD Phase Diagram. *Phys. Lett.* **2013**, *B719*, 131. [CrossRef]
22. Schaefer, B.-J.; Wambach, J. Susceptibilities near the QCD (tri)critical point. *Phys. Rev.* **2007**, *D75*, 085015. [CrossRef]
23. Schaefer, B.-J.; Pawlowski, J.M.; Wambach, J. The Phase Structure of the Polyakov-Quark-Meson Model. *Phys. Rev.* **2007**, *D76*, 074023. [CrossRef]
24. Schaefer, B.-J.; Wagner, M. On the QCD phase structure from effective models. *Prog. Part. Nucl. Phys.* **2009**, *62*, 381. [CrossRef]
25. Schaefer, B.-J.; Wagner, M.; Wambach, J. QCD thermodynamics with effective models. *PoS* **2009**, *71*, 017.
26. Weinberg, S. *Gravitation and Cosmology*; John Wiley and Sons: New York, NY, USA, 1972.
27. Parganlija, D.; Kovacs, P.; Wolf, G.; Giacosa, F.; Rischke, D.H. Meson vacuum phenomenology in a three-flavor linear sigma model with (axial-)vector mesons. *Phys. Rev.* **2013**, *D87*, 014011. [CrossRef]
28. Kovacs, P.; Wolf, G.; Giacosa, F.; Parganlija, D. Meson vacuum phenomenology in a three-flavor linear sigma model with (axial-)vector mesons. *EPJ Web Conf.* **2011**, *13*, 02006.
29. Roessner, S.; Ratti, C.; Weise, W. Polyakov loop, diquarks and the two-flavour phase diagram. *Phys. Rev.* **2007**, *D75*, 034007.
30. Lo, P.M.; Friman, B.; Kaczmarek, O.; Redlich, K.; Sasaki, C. Polyakov loop fluctuations in SU(3) lattice gauge theory and an effective gluon potential. *Phys. Rev.* **2013**, *D88*, 074502. [CrossRef]
31. Kapusta, J.I.; Gale, C. *Finite-Temperature Field Theory: Principles and Applications*; Cambridge University Press: Cambridge, UK, 2006.
32. Mao, H.; Jin, J.; Huang, M. Phase diagram and thermodynamics of the Polyakov linear sigma model with three quark flavors. *J. Phys.* **2010**, *G37*, 035001. [CrossRef]
33. Schaefer, B.-J.; Wagner, M.; Wambach, J. Thermodynamics of (2+1)-flavor QCD: Confronting Models with Lattice Studies. *Phys. Rev.* **2010**, *D81*, 074013. [CrossRef]
34. Barnett, R.M.; Carone, C.D.; Groom, D.E.; Trippe, T.G.; Wohl, C.G.; Armstrong, B.; Gee, P.S.; Wagman, G.S.; James, F.; Mangano, M.; et al. Review of Particle Physics. *Phys. Rev. D* **1996**, *54*, 1. [CrossRef]

35. Tanabashi, M.; Hagiwara, K.; Hikasa, K.; Nakamura, K.; Sumino, Y.; Takahashi, F.; Tanaka, J.; Agashe, K.; Aielli, G.; Amsler, C.; et al. Review of Particle Physics. *Phys. Rev. D* **2018**, *98*, 030001. [CrossRef]
36. Aoki, S.; Aoki, Y.; Bečirević, D.; Bernard, C.; Blum, T.; Colangelo, G.; Della Morte, M.; Dimopoulos, P.; Dürr, S.; et al. Review of lattice results concerning low-energy particle physics. *Eur. Phys. J. C* **2017**, *77*, 112. [CrossRef]
37. Tawfik, A.N.; Diab, A.M.; Ghoneim, M.T.; Anwer, H. SU(3) Polyakov Linear-Sigma Model With Finite Isospin Asymmetry: QCD Phase Diagram. *Int. J. Mod. Phys. A* **2019**, *34*, 1950199. [CrossRef]
38. Brandt, B.B.; Endrodi, G.; Schmalzbauer, S. QCD phase diagram for nonzero isospin-asymmetry. *Phys. Rev.* **2018**, *D97*, 054514. [CrossRef]
39. Cea, P.; Cosmai, L.; D'Elia, M.; Papa, A.; Sanfilippo, F. The critical line of two-flavor QCD at finite isospin or baryon densities from imaginary chemical potentials. *Phys. Rev.* **2012**, *D85*, 094512. [CrossRef]
40. Tawfik, A.N.; Diab, A.M.; Hussein, T.M. Chiral phase structure of the sixteen meson states in the SU(3) Polyakov linear-sigma model for finite temperature and chemical potential in a strong magnetic field. *Chin.Phys.C* **2019**, *43*, 034103. [CrossRef]
41. Tawfik, A.N.; Diab, A.M.; Hussein, M.T. SU(3) Polyakov linear-sigma model: Magnetic properties of QCD matter in thermal and dense medium. *J. Exp. Theor. Phys.* **2018**, *126*, 620. [CrossRef]
42. Tawfik, A.; Magdy, N.; Diab, A. Polyakov linear SU(3) σ model: Features of higher-order moments in a dense and thermal hadronic medium. *Phys. Rev.* **2014**, *C89*, 055210.
43. Schaffner-Bielich, J.; Stiele, R. The QCD Phase Transition at finite Isospin. In Proceedings of the 10th Conference on Quark Confinement and the Hadron Spectrum (Confinement X), Munich, Germany, 8–12 October 2012.
44. Beisitzer, T.; Stiele, R.; Schaffner-Bielich, J. Supernova Equation of State with an extended SU(3) Quark-Meson Model. *Phys. Rev.* **2014**, *D90*, 085001.